RSC Advances

PAPER

View Article Online
View Journal | View Issue

Cite this: *RSC Adv.*, 2016, **6**, 18654

An amperometric glucose biosensor based on a MnO_2/graphene composite modified electrode

Yuge Liu,*[a] Xiumei Zhang,[a] Dongning He,[b] Feiyue Ma,[a] Qiong Fu[a] and Yun Hu*[c]

Received 29th January 2016
Accepted 3rd February 2016

DOI: 10.1039/c6ra02680j

www.rsc.org/advances

In this paper, a novel composite of graphene/MnO_2 (GR/MnO_2) was successfully synthesized by a simple one-step hydrothermal method. The as-synthesized MnO_2 and the composite were characterized by scanning electron microscopy (SEM), X-ray diffraction (XRD), X-ray photoelectron spectroscopy (XPS) and Fourier transform infrared spectroscopy (FTIR). The results showed that MnO_2 was nanorods and the two materials were perfectly composited. The composite was decorated on a glassy carbon electrode (GCE) and used for the entrapment of glucose oxidase (GOD). Electrochemical results showed that the composite modified electrode showed a pair of well-defined redox peaks, and the direct electron transfer between GOD and the electrode surface was accelerated. The sensor fabricated by the composite modified electrode showed an excellent response to the oxidation of glucose with a wide linear range (0.04 to 2 mM), low detection limit (10 μM), and high sensitivity (3.3 μA mM^{-1} cm^{-2}). The sensor also exhibited excellent reproducibility, stability and selectivity, and it can be used in the determination of glucose in real samples.

1. Introduction

Determination of glucose is quite important in the fields of food industry, biofuel cells, textile industry, health and medical systems.[1–4] There are many approaches for the detection of glucose, among which biosensors have attracted much attention. It is reported that glucose biosensors may account for approximately 85% of the entire biosensor market. Glucose oxidase (GOD) has been widely used in glucose biosensor construction due to its highly stable structure and wide pH range of activity. Accordingly, biosensors based on the direct electrochemistry of GOD have played a leading role in glucose monitoring in the past decades.

However, the electroactive centers of GOD are embedded within the structure of biomacromolecules, and the direct electron transfer between the electroactive center and the substrate electrode is difficult to occur. Meanwhile, adsorption of the enzyme molecules onto bare electrode surface may lead to their denaturation, which also decreases direct electron transfer rate and the efficiency for glucose detection. Therefore, immobilization of GOD on supports is needed to display its special properties.

The development of materials science and nanotechnology has brought a great momentum to bioanalysis. Analysts in this field are always enthusiastic about finding new materials with good biocompatibility to improve the behavior of biosensors. Different kinds of nanomaterials, including metal nano particles,[5–7] oxides,[8,9] nanocomposites,[10,11] quantum dots,[12,13] layered materials and so on,[14–20] have been explored to modify electrodes for improving the performance of biosensors until now.

Recently, manganese dioxide (MnO_2) has received much attention due to its low-cost, beneficial physicochemical property, and relatively environmentally benign properties.[21–24] Manganese dioxide has been considered as one of the most attractive inorganic material and has been used in catalysis, molecular adsorption and energy storage. Besides, has also been widely used in biosensors.[25–28] However, the application of MnO_2 was restricted by its poor electrical conductivity.

Since the discovery by Geim *et al.*,[29] grapheme (GR) has received persistent attention. This is due to its unique electrical, mechanical, and thermal properties.[30–32] It is reported that the theoretical specific surface area of graphene can reach 2630 m^2 g^{-1}, even larger than that of a single-walled carbon nanotube (1300 m^2 g^{-1}).[33] Those special properties imply that GR has giant potential in the field of biosensors. Until now, GR has been used for the detection of dopamine, hydrogen peroxide, glucose and so on.[34–36]

Besides, the composites of GR are also getting more and more attention, especially composited with MnO_2. Those composites combine the advantages of the two materials and possess more application in different fields. Until now, composites of GR/MnO_2 with various morphologies have been

[a]Key Laboratory of Tropical Fruit Biology of Ministry of Agriculture, The South Subtropical Crop Research Institute, Chinese Academy of Tropical Agricultural Science, Zhanjiang, 524091, China. E-mail: liuyugehb@sina.com

[b]Centre of Excellence in Engineered Fibre Composites, University of Southern Queensland, Toowoomba, Qld 4350, Australia

[c]Technology Center of China Tobacco Guizhou Industrial Co. Ltd, Guiyang, 550002, China. E-mail: huyunyun99@hotmail.com

synthesized, including nanoparticles, nanowires, nanosheets, spheres and hollow spheres, nanobelts, unchinlike and so on.[21,37–42] These composites showed excellent electrochemical properties and have been mainly used in supercapacitors. However, there have been few reports on their application in biosensors.[43,44]

Here in this research, MnO_2 nanorods and the composite of GR/MnO_2 were synthesized by a simple and facile hydrothermal method. Scanning electron microscopy (SEM), X-ray diffraction (XRD), X-ray photoelectron spectroscopy (XPS), and Fourier transform infrared spectroscopy (FTIR) were used to investigate the structure and morphologies of MnO_2 and the GR/MnO_2 composite. Furthermore, the composite was used for the modification of glassy carbon electrode (GCE) and glucose oxidase (GOD) was entrapped. The direct electron transfer between GOD and the electrode can be easily realized and the biosensor fabricated showed excellent response to glucose detection. The composite modified electrode can also be used for the determination of glucose in real serums.

2. Experimental

Chemicals and reagents

Natural graphite flake (about 325 mesh) used for the synthesis of graphene oxide (GO) was purchased from Alfa Aesar Chemical Reagent Co. Manganese sulfate ($MnSO_4 \cdot H_2O$) and ammonium persulfate (APS) were purchased from Shanghai Chemical Reagent Co. GOD (Type VII from Aspergillus nige, 196 000 units per g of solid) was obtained from Sigma-Aldrich Chemical Co. and used as received. All other reagents were of analytical grade and used without further purification.

Synthesis of MnO_2 nanorods and GR/MnO_2 composite

GO was constructed by the modified Hummers method described previously.[45] The GR/MnO_2 composite was synthesized by a one-step hydrothermal method. The weight ratio of GO to MnO_2 was varied as 2 : 1, 1 : 1, 1 : 2, and 1 : 3, and the corresponding composites were named as GM-1, GM-2, GM-3, and GM-4. The typical synthesis of GM-1 was as follows: 2 mg mL/1 GO dispersion was prepared by sonication of 20 mg GO in 10 mL of water. 20 mg of manganese sulfate was scattered into 5 mL water and then the solution was added into the above GO dispersion drop by drop. After stirring for 30 min, the mixture was transferred into a Teflon-lined stainless steel autoclave and heated at 170 °C for 20 h. When there was no GO in the reaction, MnO_2 nanorods were synthesized.

Preparation of GR/MnO_2 composite modified electrodes

GCE was first polished with 1.0, 0.3, and 0.05 μm alumina slurry successively and followed by rinsing with doubly distilled water and drying at room temperature. The GR/MnO_2 composite was dispersed in distilled water to form a 2.0 mg mL^{-1} solution under ultrasonication. The resultant colloidal solution (5 μL) was then dropped onto the pretreated electrode surface and allowed to dry under ambient conditions. For the direct electron transfer of GOD, 5 mg mL^{-1} GOD and 0.5% Nafion were subsequently cast onto the GR/MnO_2 composite modified GCE and allowed to dry under ambient conditions for 2 h after each dropcasting step.

Instruments

The morphologies of MnO_2 and the GR/MnO_2 composite were investigated by scanning electron microscopy (SEM, S4800). X-ray diffraction (XRD) patterns were determined by a Philip-X'Pert X-ray diffractometer with Cu Kα radiation ($\lambda = 1.5418$ Å).

X-ray photoelectron spectroscopy (XPS) was performed on ESCA-LAB MK II X-ray photoelectron spectrometer. Fourier transform infrared (FTIR) spectroscopic measurements were taken on a Bruker model VECTOR22 Fourier transform spectrometer. Zeta potential analysis was measured on a PALS/90plus analyzer.

Cyclic voltammetric and amperometric experiments were conducted with a CHI660B workstation (Shanghai Chenhua, Shanghai). All experiments were carried out using a conventional three-electrode system in 0.1 M phosphate buffer solution (PBS), where composite modified GCE was used as the working electrode, a platinum wire as the auxiliary electrode and a saturated calomel electrode (SCE) as the reference electrode. All solutions were deoxygenated by highly pure nitrogen before and during the measurements except for the determination of glucose.

3. Results and discussion

Characterization of MnO_2 nanorods and the GR/MnO_2 composite

SEM results showed that the diameter of as-prepared MnO_2 nanorods varies from 60 to 100 nm with an average length up to 1–4 μm (Fig. 1A). The nanorods were well dispersed, which makes them easier to spread on the surface of GR. According to the report, GO was highly negatively charged due to the large amounts of oxygen-containing functional groups on the surface and edges of the GO nanosheets.[21] In the reaction solution of synthesizing the composite, Mn^{2+} was adsorbed on the surface and edges of the GO by electrostatic forces and then oxidized by oxidant. The chemical reaction involved in the synthesis of MnO_2 and the composite is as follows:[46]

$$MnSO_4 + (NH_4)_2S_2O_8 + 2H_2O \rightarrow MnO_2 + (NH_4)_2SO_4 + 2H_2SO_4 \quad (1)$$

Which may comprise two half reactions:

$$Mn^{2+} + 2H_2O \rightarrow MnO_2 + 4H^+ + 2e \ (E^\circ = 1.23\ V) \quad (2)$$

$$S_2O_8^{2-} + 2e \rightarrow 2SO_4^{2-} \ (E^\circ = 2.01\ V) \quad (3)$$

The original weight ratio of GO to MnO_2 showed great impact on the morphologies of the GR/MnO_2 composite. When the weight ratio was 2 : 1, about half of the GR surface can not be reached by nanorods (Fig. 1B). With the increase of MnO_2 in the reaction mixture, more nanorods were attached. However,

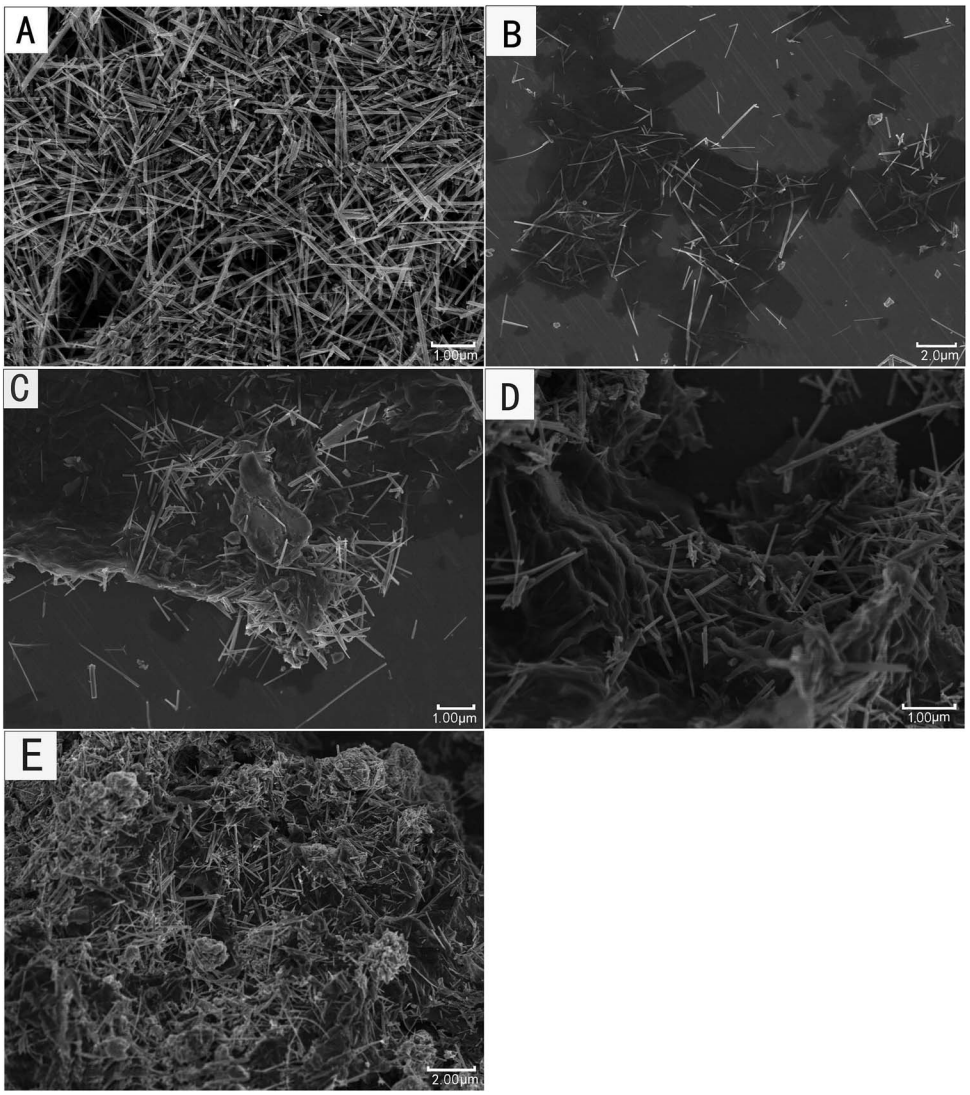

Fig. 1 SEM images (A) β-MnO_2 nanorods; (B) GM-1; (C) GM-2; (D) GM-3 and (E) GM-4.

when the ratio reaches 1 : 3, some nanorods also could not spread onto the surface of GR because there were too many of them (Fig. 1E). The perfect weight ratio was 1 : 2 for the synthesis of GR/MnO_2 composite (Fig. 1D).

The crystalline phase of the as-prepared samples was determined by XRD measurements. All of the diffraction peaks of MnO_2 (Fig. 2A) in the spectrum can be indexed to the tetragonal phase of β-MnO_2 with lattice constants a = 4.3999 Å and c = 2.8740 Å (JCPDS 24-0735). The peaks centered at about 28.7, 37.47, 56.73 and 72.54° can be indexed to (110), (101), (211) and (301). The other peaks can be indexed to (200), (111), (210), (220), (002), (310) and (301). The main peaks were narrow and high, suggesting high crystallinity. No other characteristic reflections were detected, indicating that there were no impurities in the as-synthesized material. The peaks of MnO_2 were also found in the diffraction spectrum of the composite at the same location (Fig. 2B), which indicated that GR and MnO_2 were well composited.

XPS measurement was performed in order to study the chemical composition of the composite. It can seen from Fig. 2B that the peaks of Mn $2p_{3/2}$ and Mn $2p_{1/2}$ were centered at 642.1 eV and 653.8 eV respectively, and the spin-energy separation was 11.7 eV. The data agree well with that reported, which indicated that the Mn elements were in the form of Mn(IV) in the composite.[47]

The composition was also investigated by FTIR. In the case of pure GO (Fig. 3a), the adsorption peaks at about 1730 cm^{-1} and 1380 cm^{-1} are associated with vibration of the C=O bond of carboxylic groups and O=C–O from carboxylate. The bands of stretching vibrations at 1225 and 1052 cm^{-1} correspond to epoxy and alkoxy C–O groups, respectively. In addition, the broad absorption band at 3420 cm^{-1} can be assigned to the O–H stretching vibration of water molecule. The intensities of characteristic absorption peaks of GO were dramatically decreased in the GR/MnO_2 composite (Fig. 3b). At the same time, the intensity of –C=C– absorption peak at 1575 cm^{-1} is enhanced, indicating the conversion of GO to GR.

Zeta potentials of GO and GR were also detected, and the results were −35 and −10 mV, respectively. This showed that the two materials possessed favorable dispersibility.

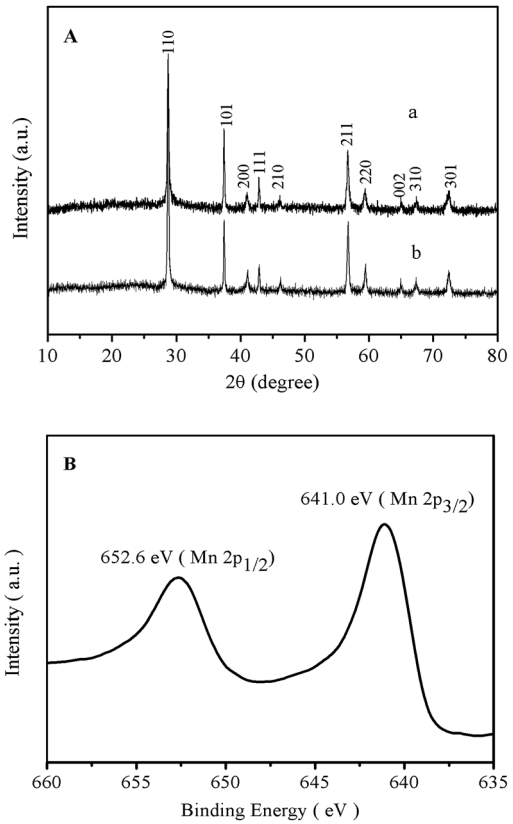

Fig. 2 (A) XRD patterns of (a) β-MnO_2 nanorods and (b) GR/MnO_2 composite; (B) XPS survey spectra of the GR/MnO_2 composite.

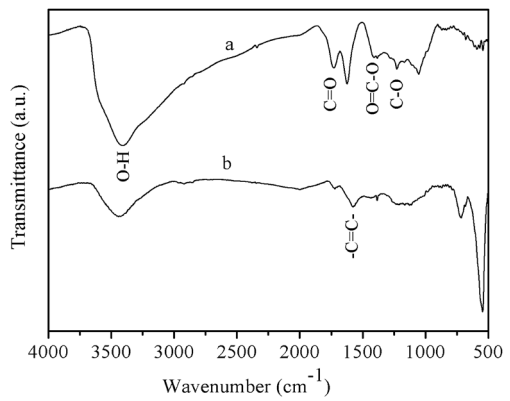

Fig. 3 FTIR spectra of (a) GO and (b) GR/MnO_2 composite.

Besides, GR carried less negatively charge than that of GO, indicating the conversion of GO to GR, and this was in accordance with the results of FTIR.

Entrapment of GOD onto the GR/MnO_2 composite modified electrode

As mentioned by Yin *et al.*, MnO_2 can act as a catalyst to the decomposition of hydrogen peroxide, and the oxygen produced can be used for the oxidation of glucose, this makes this material applicable in constructing glucose biosensor.[28] However, the poor electrical conductivity of MnO_2 restricts its application. It is well known that GR is biocompatible and highly conductive. The composition of the two materials will definitely result in better sensitivity in biosensors. Based on the advantages of both MnO_2 and GR, the composite is quite suitable for the construction of biosensors. Therefore, the GR/MnO_2 composite was decorated onto the surface of GCE and GOD was entrapped. The corresponding electrochemical properties were investigated in detail.

Direct electrochemistry of GR/MnO_2/GOD/Nafion modified electrode

The cyclic voltammograms (CVs) of different electrodes in pH 7.0 PBS at 100 mV s^{-1} are given in Fig. 4A. The GR/MnO_2/Nafion modified electrode did not show any obvious redox peaks (curve a), indicating that the Nafion membrane and the GR/MnO_2 composite are not electroactive in this potential range. After the entrapment of GOD, the GR/MnO_2/GOD/Nafion modified electrode shows a pair of well-defined redox peaks at −0.38 and −0.4 V (curve c), respectively. The GOD/Nafion modified electrode shows no peaks (curve b), which may be due to the slow

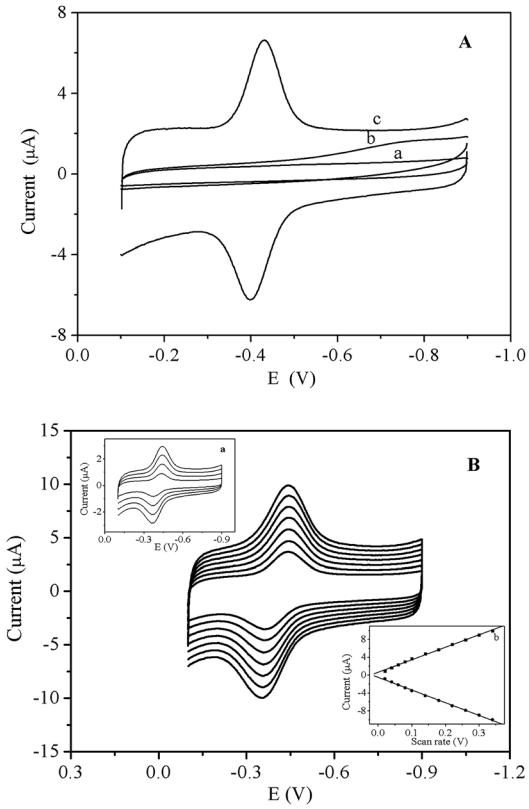

Fig. 4 (A) Cyclic voltammograms of (a) GR/MnO_2/Nafion, (b) GOD/Nafion, (c) GR/MnO_2/GOD/Nafion modified GCE in 0.1 M air-free pH 6.0 PBS at 100 mV s^{-1}. (B) Cyclic voltammograms of GR/MnO_2/GOD/Nafion modified GCE in 0.1 M air-free pH 6.0 PBS at scan rates of 100, 140, 180, 220, 260, 300, and 340 mV s^{-1} (from inner to outside), inset (a) GR/MnO_2/GOD/Nafion modified GCE at the scan rates of 20, 40, 60, 80 mV s^{-1} (from inner to outside). (b) Plots of the anodic and cathodic peak currents *vs.* scan rate.

electron transfer of GOD at the electrode. Thus, the GR/MnO_2 composite is very effective in the realization of the direct electron transfer of GOD molecules.

The electrode shows a couple of well-defined peaks at different scan rates (Fig. 4B). With the increase of scan rate, the redox peak currents of the GOD increased linearly (inset of Fig. 4B, b). According to the research of Laviron, the electrode reaction is a surface confined process.[48]

From Faraday's law, the average surface coverage of GOD is calculated to be 1.75×10^{-10} mol cm^{-2}. The saturated monolayer surface coverage of GOD on the electrode was reported to be 1.7×10^{-12} mol cm^{-2}.[49] The value of 1.75×10^{-10} mol cm^{-2} in this research was much larger than that reported. Therefore, GOD is of multilayer on the GR/MnO_2/Nafion modified electrode.

Small peak-to-peak separation always indicates a fast electron transfer rate. The electron transfer rate constant k_s can be estimated by the Laviron equation:[50]

$$k_s = mnFv/RT$$

In the formula, m is a parameter related to the peak-to-peak separation, T is the temperature, n is the number of electrons, v is the scan rate, F is the Faraday's constant, and R is the gas constant. The constant of k_s estimated from the formula is $2.57 \pm 0.39\ s^{-1}$. This value is much larger than that of GOD adsorbed on Au NPs and Nafion film ($1.3\ s^{-1}$), Nafion-CNT/GC electrode ($1.53 \pm 0.45\ s^{-1}$), and that of gold electrode modified with 3,3′-dithiobissulfocinnimidylpropionate ($0.026\ s^{-1}$).[51–53] This further suggests that the GR/MnO_2 composite provides an excellent biocompatible environment for GOD and facilitates the electron transfer reaction.

Influence of solution pH on the direct electron transfer of GOD

The pH value of solution is very essential to the electrochemical behaviors of biomolecules in most cases. In this research, the GR/MnO_2/GOD/Nafion modified electrode shows strong dependence on the pH value of solution. In general, all changes in the peak potentials and currents with solution pH were reversible in the pH range from 4.0 to 7.0.

With the increase of pH, the formal potential exhibited a linear relationship *versus* pH with a slope of -53.6 mV pH^{-1} (Fig. 5A). The value is quite close to the theoretical value of -59.0 mV pH^{-1} corresponding to the conversion between GOx (FAD) and GOx. All of these indicate that two protons ($2H^+$) and two electrons ($2e^-$) participate in the direct electrochemical reaction of GOD immobilized on GR/MnO_2/GOD/Nafion modified electrode.

Application of the GR/MnO_2/GOD/Nafion modified electrode in biosensing

The CVs of GR/MnO_2/GOD/Nafion modified electrodes in nitrogen- and air-saturated 0.1 M pH 6.0 PBS are given in Fig. 5B. A pair of well defined redox peaks can be observed in both nitrogen and air-saturated PBS (curve a and c). However, the reduction peak current in air-saturated PBS is larger than that in nitrogen-saturated solution, which indicates that GOD can electrocatalyze the reduction of the dissolved oxygen as follows:

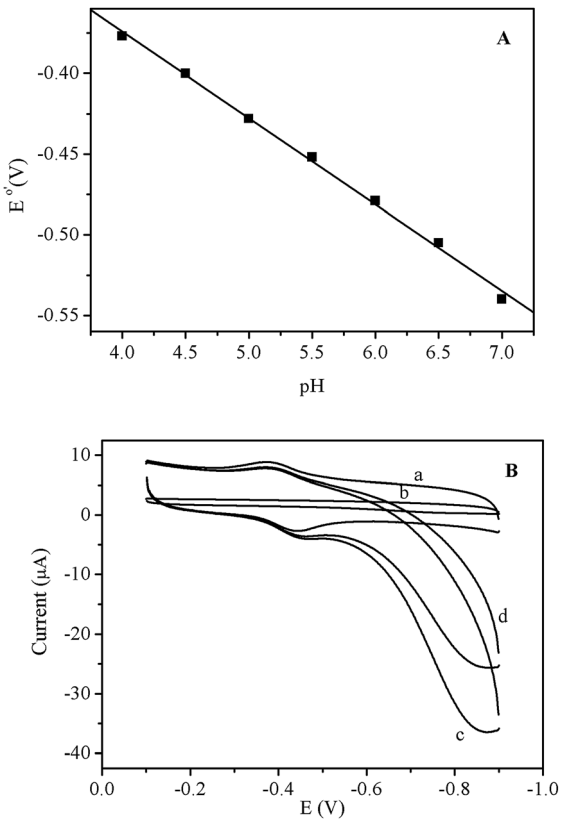

Fig. 5 (A) Plot of the formal potential *vs.* pH; (B) cyclic voltammograms of (a) GR/MnO_2/GOD/Nafion modified electrode in air-free 0.1 M pH 6.0 PBS; (b) GR/MnO_2/Nafion modified electrode in air-saturated 0.1 M pH 6.0 PBS with 2 mM glucose; (c) GR/MnO_2/GOD/Nafion modified electrode in air-saturated PBS without glucose and (d) with 1 mM glucose at 100 mV s^{-1}.

$$GOD\text{–}FADH_2 + O_2 \rightarrow GOD\text{–}FAD + H_2O_2 \quad (4)$$

With the addition of glucose to the air-saturated PBS, the GR/MnO_2/Nafion modified electrode shows no response (Fig. 5B, curve b), indicating that GR/MnO_2 cannot catalyze the oxidation of glucose. However, the reduction peak current decreases at the GR/MnO_2/GOD/Nafion modified electrode (Fig. 5B, curve d), indicating that GOD remains its bioelectrocatalytic activities and can catalyze the oxidation of glucose by consuming the oxygen molecular oxygen of the dissolved oxygen. On the basis of the decrease of the electrocatalytic response, this system can be used to construct a biosensor for glucose detecting.

The effects of solution pH and temperature on the amperometric response were investigated. It can be seen from Fig. 6 that the optimal values of the two parameters were pH 6.0 and 35 °C.

Shown in Fig. 7 is a typical amperometric response curve of the biosensor through successive injections of glucose to stirring air-saturated pH 6.0 PBS at 35 °C. It can be clearly seen that

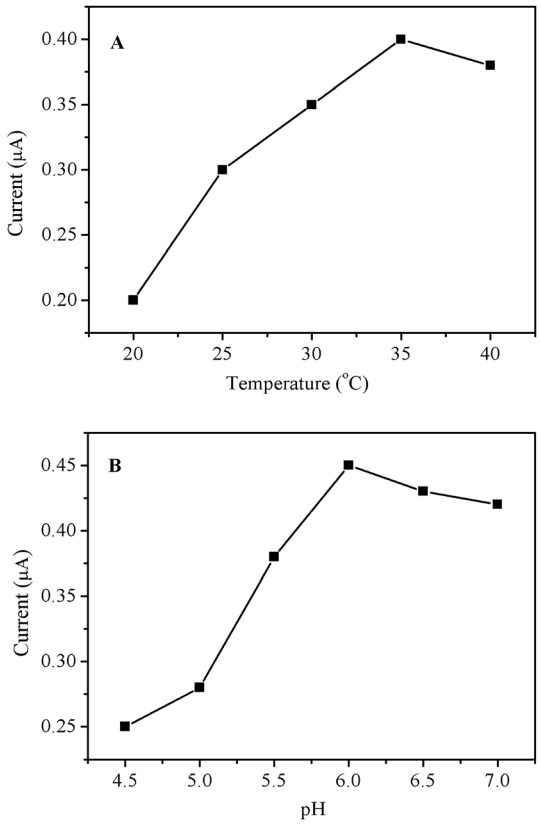

Fig. 6 Effects of (A) temperature and (B) solution pH values on the amperometric response of the GR/MnO_2/Nafion modified electrode.

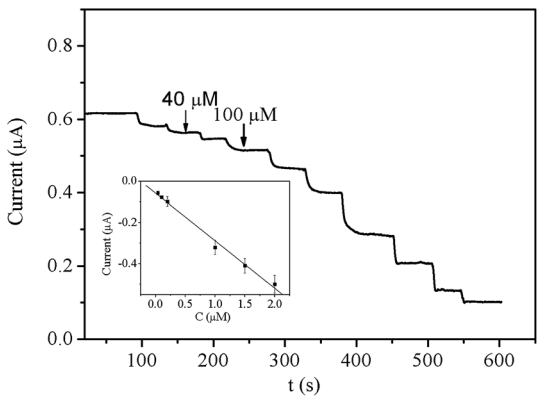

Fig. 7 Amperometric response curve of the GR/MnO_2/Nafion modified electrode for successive additions of specific concentrations of glucose to air-saturated 0.1 M pH 6.0 PBS under stirring at −0.38 V and 35 °C. Inset: linear plot of current *vs.* glucose concentration.

the reduction current successively decreases with the addition of glucose. The biosensor achieved 90% of the steady-state current within 10 s, indicating a quick response process. The linear calibration range for glucose is 0.04–2 mM (inset of Fig. 7, $n = 6$, $R^2 = 0.996$). The limit of detection (LOD) calculated by the equation of $3S_B/b$ was 10 μM, where S_B and b present the standard deviation of the blank solution and the slope of the analytical curve, respectively.[43] The detection limit is much lower than that of the GOx–PLL/RGO–ZrO_2 composite film modified electrode.[43] The sensitivity of the biosensor calculated from the slope of the calibration plot was 3.3 μA mM^{-1} cm^{-2}.

The performance of the GR/MnO_2/GOD/Nafion modified electrode was compared with those reported (Table 1). The results showed that the electrode possessed high sensitivity.

Stability and reproducibility

Additional experiments were carried out to test the reproducibility and stability of the composite modified electrode. No obvious change could be seen from the CV curves after 100 cyclic scans in pH 7.0 PBS at 100 mV s^{-1}. The biosensor was stored at 4 °C when not used. It retained about 90% of its original sensitivity after two weeks, indicating a good stability.

The relative standard deviation (RSD) of the peak current in six successive determinations on one electrode at a glucose concentration of 0.5 mM was 2.7% for the GR/MnO_2/GOD/Nafion modified GCE. Six different modified electrodes were independently fabricated and the corresponding RSD value for the determination of 0.5 mM glucose was 5%.

Interference and serum sample analysis

The biosensor also shows a good selectivity for glucose. In an air-saturated and stirred 0.1 M pH 6.0 PBS containing 1 mM glucose, the response arising from 0.1 mM uric acid (UA) and ascorbic acid (AA) is negligible. This may be contributed to the use of Nafion during the preparation of modified electrodes.

The GR/MnO_2/GOD/Nafion modified electrode was also used for the determination of glucose in real human serum samples. The serum samples were diluted with pH 6.0 PBS in advance. The values detected by the electrode and provided by the hospital were given in Table 2. The recoveries for the electrochemical assays of 0.5–1 mM glucose were between 93% and

Table 1 Performance comparison of the proposed GR/MnO_2/Nafion modified electrode with other glucose sensors

Material	Detection limit (μM)	Sensitivity (μA mM^{-1} cm^{-2})	Ref.
PVA/MnO_2@GO/CuO	—	—	54
TiO_2–graphene	—	—	55
GOD–Aunano–DHP	100	1.14	56
Silica sol–gel–GOx–CNTs	50	0.196	57
Nafion/GOD–OMCs	53	0.053	58
R/MnO_2/GOD/Nafion	10	3.3	This work

Table 2 Determination of glucose in real samples

Samples	Values provided by the hospital	Determined by the modified electrode	Relative error (%)
1	5.5	5.3	−3.62
2	6.5	6.3	−3.07
3	4.8	4.9	2.08

105%, indicating that the fabricated glucose biosensor has potential in practical application.

4. Conclusions

In this research, the composite of GR/MnO_2 nanorods were synthesized by a simple and facile hydrothermal method. Controlled experiments demonstrated the perfect weight ratio value of GO to MnO_2 was 1 : 2 for the best morphology. The composition combined the original high crystalline phase of MnO_2 and the excellent conducting properties of the two materials. The composite was used for the decoration of GCE and GOD was entrapped. Electrochemical results showed the direct electrochemistry of GOD was realized with a fast electrontransfer rate. The biosensor fabricated by the composite modified electrode showed excellent response to the oxidation of glucose, and it can also be used to determine glucose in real samples with negligible interference from uric acid and ascorbic acid by using Nafion as binder. The investigation here has provided not only a facile way for realization of direct electrochemistry of GOD but also a fast determination of glucose in real samples.

Acknowledgements

This work is supported by the National Natural Science Foundation of China (No. 21505155), and the Natural science Foundation of Hainan province (No. 20153122).

Notes and references

1 C. M. Wong, K. H. Wong and X. D. Chen, *Appl. Microbiol. Biotechnol.*, 2008, **78**, 927–938.
2 S. B. Bankar, M. V. Bule, R. S. Singhal and L. Ananthanarayan, *Biotechnol. Adv.*, 2009, **27**, 489–501.
3 Y. T. Wang, L. Yu, Z. Q. Zhu, J. Zhang, J. Z. Zhu and C. H. Fan, *Sens. Actuators, B*, 2009, **136**, 332–337.
4 A. Heller and B. Feldman, *Chem. Rev.*, 2008, **108**, 2482–2505.
5 H. Wang, X. Wang, X. Zhang, X. Qin, Z. Zhao, Z. Miao, N. Huang and Q. Chen, *Biosens. Bioelectron.*, 2009, **25**, 142–146.
6 W. Jia, K. Wang, Z. Zhu, H. Song and X. Xia, *Langmuir*, 2007, **23**, 11896–11900.
7 C.-W. Hsu and G.-J. Wang, *Biosens. Bioelectron.*, 2014, **56**, 204–209.
8 T. Kong, Y. Chen, Y. Ye, K. Zhang, Z. Wang and X. Wang, *Sens. Actuators, B*, 2009, **138**, 344–350.
9 M. Zhao, Z. Li, Z. Han, K. Wang, Y. Zhou, J. Huang and Z. Ye, *Biosens. Bioelectron.*, 2013, **49**, 318–322.
10 Y. Liu, X. Feng, J. Shen, J.-J. Zhu and W. Hou, *J. Phys. Chem. B*, 2008, **112**, 9237–9242.
11 S. Palanisamy, S. Cheemalapati and S.-M. Chen, *Biosens. Bioelectron.*, 2010, **26**, 504–510.
12 H. Dhyani, M. A. Ali, M. K. Pandey, B. D. Malhotra and P. Sen, *J. Mater. Chem.*, 2012, **22**, 4970–4976.
13 X. Meng, J. Wei, X. Ren, J. Ren and F. Tang, *Biosens. Bioelectron.*, 2013, **47**, 402–407.
14 Y.-G. Liu, C. B. Wei, L.-L. Lv and S.-H. Liu, *J. Solid State Electrochem.*, 2012, **16**, 2211–2216.
15 W. Sun, Y. Guo, Y. Lu, A. Hu, F. Shi, T. Li and Z. Sun, *Electrochim. Acta*, 2013, **91**, 130–136.
16 Y. Liu, C. Lu, W. Hou and J.-J. Zhu, *Anal. Biochem.*, 2008, **375**, 27–34.
17 J. Singh, P. Kalita, M. K. Singh and B. D. Malhotra, *Appl. Phys. Lett.*, 2011, **98**, 123702.
18 J. Singh, P. Kalita, T. Kuila, M. Srivastava, A. K. Das, N. H. Kim, B. J. Jung, D. Y. Kim, S. H. Lee, D. Won Lee, D.-G. Kim and J. H. Lee, *Process Biochem.*, 2013, **48**, 1724–1735.
19 J. Singh, A. Roychoudhury, M. Srivastava, V. Chaudhary, R. Prasanna, D. W. Lee, S. H. Lee and B. D. Malhotra, *J. Phys. Chem. C*, 2013, **117**, 8491–8502.
20 J. Singh, A. Roychoudhury, M. Srivastava, P. R. Solanki, D. W. Lee, S. H. Lee and B. D. Malhotra, *Nanoscale*, 2014, **6**, 1195–1208.
21 X. Feng, Z. Yan, N. Chen, Y. Zhang, Y. Ma, X. Liu, Q. Fan, L. Wang and W. Huang, *J. Mater. Chem. A*, 2013, **1**, 12818–12825.
22 B. S. Ljukic and R. G. Compton, *Electroanalysis*, 2007, **19**, 1275–1280.
23 M.-T. Lee, C.-Y. Fan, Y.-C. Wang, H.-Y. Li, J.-K. Chang and C.-M. Tseng, *J. Mater. Chem. A*, 2013, **1**, 3395–3405.
24 Y. Munaiah, B. G. S. Raj, T. P. Kumar and P. Ragupathy, *J. Mater. Chem. A*, 2013, **1**, 4300–4306.
25 L. Zhang, Z. Fang, Y. Ni and G. Zhao, *Int. J. Electrochem. Sci.*, 2009, **4**, 407–413.
26 M. Yoshimoto, C. Iida, A. Kariya, N. Takaki and M. Nakayama, *Electroanalysis*, 2010, **22**, 653–659.
27 Z. Zhu, L. Qu, Q. Niu, Y. Zengand and X. Huang, *Biosens. Bioelectron.*, 2011, **26**, 2119–2124.
28 L.-T. Yin, J.-C. Chou, W.-Y. Chung, T.-P. Sun, K.-P. Hsiung and S.-K. Hsiung, *Sens. Actuators, B*, 2001, **76**, 187–192.
29 A. K. Geim and K. S. Novoselov, *Nat. Mater.*, 2007, **6**, 183–191.
30 B. Luo, S. Liu and L. Zhi, *Small*, 2012, **8**, 630–646.
31 Y. Chen, B. Zhang, G. Liu, X. Zhang and E. T. Kang, *Chem. Soc. Rev.*, 2012, **41**, 4688–4707.
32 Y. B. Tan and J.-M. Lee, *J. Mater. Chem. A*, 2013, **1**, 14814–14843.
33 S. Stankovich, D. A. Dikin, G. H. Dommett, K. M. Kohlhaas, E. J. Zimney, E. A. Stach, R. D. Piner, S. T. Nguyen and R. S. Ruoff, *Nature*, 2006, **442**, 282–286.
34 B. Zhao, Z. R. Liu, W. Y. Fu and H. B. Yang, *Electrochem. Commun.*, 2013, **27**, 1–4.
35 J. W. Wu, C. H. Wang, Y. C. Wang and J. K. Chang, *Biosens. Bioelectron.*, 2013, **46**, 30–36.
36 N. German, A. Kausaite-Minkstimiene, A. Ramanavicius, T. Semashko, R. Mikhailova and A. Ramanaviciene, *Electrochim. Acta*, 2015, **169**, 326–333.
37 X. Zhao, B. M. Sanchez, P. J. Dobson and P. S. Grant, *Nanoscale*, 2011, **3**, 839–855.
38 S. Chen, J. Zhu, X. Wu, Q. Han and X. Wang, *ACS Nano*, 2010, **4**, 2822–2830.
39 H. Chen, S. Zhou, M. Chen and L. Wu, *J. Mater. Chem.*, 2012, **22**, 25207–25216.

40 X. Feng, N. Chen, Y. Zhang, Z. Yan, X. Liu, Y. Ma, Q. Shen, L. Wang and W. Huang, *J. Mater. Chem. A*, 2014, **2**, 9178–9184.
41 S. Zhu, H. Zhang, P. Chen, L.-H. Nie, C.-H. Li and S.-K. Li, *J. Mater. Chem. A*, 2015, **3**, 1540–1548.
42 S. Cui, Y. Li, D. Deng, L. Zeng, X. Yan, J. Qian and L. Luo, *RSC Adv.*, 2016, **6**, 2632–2640.
43 A. T. Ezhil Vilian, S.-M. Chen, M. Ajmal Alib and F. M. A. Al-Hemaid, *RSC Adv.*, 2014, **4**, 30358–30367.
44 W. Sun, X. Wang, H. Zhu, X. Sun, F. Shi, G. Li and Z. Sun, *Sens. Actuators, B*, 2013, **178**, 443–449.
45 X.-M. Feng, R.-M. Li, Y.-W. Ma, R.-F. Chen, N.-E. Shi, Q.-L. Fan and W. Huang, *Adv. Funct. Mater.*, 2011, **21**, 2989–2996.
46 X. Wang and Y. Li, *J. Am. Chem. Soc.*, 2002, **124**, 2880–2881.
47 Z. Su, C. Yang, C. Xu, H. Wu, Z. Zhang, T. Liu, C. Zhang, Q. Yang, B. Li and F. Kang, *J. Mater. Chem. A*, 2013, **1**, 12432–12440.
48 E. Laviron, *J. Electroanal. Chem.*, 1979, **100**, 263–270.
49 C. Bourdillon, C. Demaille, J. Cueris, J. Moiroux and J.-M. Savéant, *J. Am. Chem. Soc.*, 1993, **115**, 12264–12269.
50 E. Laviron, *J. Electroanal. Chem.*, 1979, **101**, 19–28.
51 S. Zhao, K. Zhang, Y. Bai, W. Yang and C. Sun, *Bioelectrochemistry*, 2006, **69**, 158–163.
52 C. X. Cai and J. Chen, *Anal. Biochem.*, 2004, **332**, 75–83.
53 L. Jiang, C. J. McNeil and J. M. Cooper, *Chem. Commun.*, 1995, 1293–1295.
54 M. M. Farid, L. Goudini, F. Piri, A. Zamani and F. Saadati, *Food Chem.*, 2016, **194**, 61–67.
55 H. D. Jang, S. K. Kim, H. Chang, K.-M. Roh, J.-W. Choi and J. Huang, *Biosens. Bioelectron.*, 2012, **38**, 184–188.
56 Y. Wu and S. Hu, *Bioelectrochemistry*, 2007, **70**, 335–341.
57 S. H. Lim, J. Wei, J. Lin, Q. Li and J. K. You, *Biosens. Bioelectron.*, 2005, **20**, 2341–2346.
58 M. Zhou, L. Shang, B. Li, L. Huang and S. Dong, *Biosens. Bioelectron.*, 2008, **24**, 442–447.